

Role of Apoptosis in the Disappearance of Infiltrated and Proliferated Interstitial Cells After Myocardial Infarction

Genzou Takemura, Michiya Ohno, Yukihiro Hayakawa, Jun Misao, Motoo Kanoh, Atsuko Ohno, Yoshihiro Uno, Shinya Minatoguchi, Takako Fujiwara, Hisayoshi Fujiwara

Abstract—Myocardial infarction (MI) progresses from the acute death of myocytes and the infiltration of inflammatory cells into granulation, followed by scars. During the healing process, the myocardial interstitial cell population in the infarcted tissues increases markedly and then decreases. We postulated that apoptosis is responsible for this process. Twenty-four male Japanese white rabbits underwent a 30-minute occlusion of the left coronary artery followed by reperfusion for 2 days, 2 weeks, or 4 weeks ($n=8$ each). The histological features consisted of dead cardiomyocytes and marked leukocyte infiltration at 2 days after MI and granulation consisting of numerous α -smooth muscle actin–positive myofibroblasts, macrophage antigen–positive macrophages, and neovascularization at 2 weeks. At 4 weeks, the cellularity decreased markedly, and scars were evident. Interstitial cells with positive nick end labeling were significantly more frequent at the light microscopic level in the 2-day MI samples ($5.3 \pm 3.6\%$ in the center and $6.9 \pm 3.3\%$ in the periphery of the infarct region) than in the 2-week ($2.5 \pm 1.0\%$) and 4-week ($0.5 \pm 0.5\%$) samples. DNA electrophoresis showed a clear ladder in tissues from the ischemic areas at 2 days after MI but not at 2 and 4 weeks after MI. Ultrastructurally, typical apoptotic figures, including apoptotic bodies and condensed nuclei without ruptured plasma membranes, were detected in leukocytes from all hearts with 2-day MI and in myofibroblasts, endothelial cells, and macrophages from all hearts with 2-week MI. In the electron microscopic in situ nick end labeling, immunogold particles intensely labeled the condensed chromatin of the typical apoptotic nuclei. These particles were also accumulated on nuclei of the interstitial cells showing homogeneous density but not definite condensation as typical apoptotic nuclei, suggesting an early stage of apoptosis. Thus, apoptosis plays an important role in the disappearance of both the infiltrated leukocytes and the proliferated interstitial cells after MI. This finding may have therapeutic implications for postinfarct ventricular remodeling through apoptosis handling during the healing stage of MI. (*Circ Res.* 1998;82:1130-1138.)

Key Words: programmed cell death ■ myocardial infarction ■ healing ■ myofibroblast

Cell death is classified into necrosis and apoptosis.¹⁻³ After MI, the myocardial tissue responds with an acute inflammatory reaction after the death of cardiomyocytes and repair, terminating with the establishment of a permanent scar. During the acute inflammatory phase, numerous acute inflammatory cells invade the dead tissue. Next, the acutely inflamed tissue is replaced by granulation tissue that is still comparatively rich in cells, including granulation tissue fibroblasts (myofibroblasts), macrophages, and small vessel cells. This evolves into scar tissue with sparse cellular components. During the transition from acute inflammation to granulation to scar tissue, the interstitial cellular population decreases markedly. Many investigators have reported that apoptosis, as well as necrosis, is associated with cardiomyocyte death in acute MI.⁴⁻¹⁰ Apoptosis-related factors such as Bcl-2 and Bax are expressed in the cardiomyocytes during ischemia.^{11,12} However, the number of precise studies on the

disappearance of the various types of proliferated interstitial cells after MI is limited. We hypothesized that apoptosis is important in the disappearance of these cells. Recently, the presence of apoptosis of the salvaged cardiomyocytes has been reported in dogs¹² and rats¹³ with old MI. It had not been determined at that time whether apoptosis of the salvaged myocytes is present in rabbits.

Apoptosis has characteristic morphological and biochemical features.^{1-3,14,15} Morphological apoptosis defined by electron microscopy includes the condensation and fragmentation of the nucleus, the modification of cytoplasmic organelles and apoptotic bodies, and the removal of apoptotic cells through phagocytosis, by macrophages or neighboring cells.¹⁻³ The key biochemical feature of apoptosis is DNA fragmentation at nucleosomal units induced by an endogenous endonuclease.^{14,15} This can be detected by DNA agarose gel electrophoresis (DNA ladders) and TUNEL at the light

Received October 20, 1997; accepted March 4, 1998.

From the Second Department of Internal Medicine (G.T., M.O., Y.H., J.M., M.K., A.O., Y.U., S.M., H.F.), Gifu University School of Medicine, Gifu, Japan, and the Department of Food Science (T.F.), Kyoto Women's University, Kyoto, Japan.

Correspondence to Hisayoshi Fujiwara, MD, Second Department of Internal Medicine, Gifu University School of Medicine, 40 Tsukasa-Machi, Gifu 500-8705, Japan.

E-mail gifuim-gif@umin.u-tokyo.ac.jp

© 1998 American Heart Association, Inc.

Selected Abbreviations and Acronyms

HPF	= high-power field
MI	= myocardial infarction
TdT	= terminal deoxynucleotidyl transferase
TUNEL	= in situ nick end labeling

microscopic level. The precise relationship between the characteristic ultrastructural features (which are morphological markers of apoptosis) and DNA fragmentation (a biochemical marker of apoptosis) in apoptotic cells in hearts was yet to be determined.

Therefore, the present study had two purposes: (1) to test whether apoptosis is associated with the disappearance of the infiltrated and proliferated interstitial cells and whether it is present in the salvaged myocytes after MI in rabbits and (2) to elucidate the relationship between the ultrastructure of apoptotic cells and DNA fragmentation using the electron microscopic TUNEL method.

Materials and Methods

In the present study, all rabbits received humane care in accordance with the *Guide for the Care and Use of Laboratory Animals* published by the US National Institutes of Health (NIH publication No. 8523, revised 1985).

Materials and Experimental Procedures

A total of 24 male Japanese white rabbits weighing 1.7 to 2.3 kg underwent MI. The anterolateral branch of the coronary artery was occluded for 30 minutes and then reperfused for 2 days, 2 weeks, or 4 weeks (n=8 each).

Rabbits were anesthetized by an intravenous injection of pentobarbital sodium (30 to 40 mg/kg), and additional doses were given when required throughout the experiment. They were orally intubated and mechanically ventilated with room air supplemented with a low flow of oxygen (tidal volume, 25 to 35 mL; respiration rate, 20 to 30 breaths/min). The respirator was adjusted on the basis of the results of a serial arterial blood gas analysis to maintain arterial blood gases within the physiological range. The standard limb leads of the ECG were monitored. The surgery was conducted under sterile conditions. A catheter was placed in the right carotid artery for blood gas and blood pressure monitoring. The rabbits were then systemically heparinized (500 U/kg). The chest was opened via a left thoracotomy, the pericardium was opened, and the heart was exposed. A 4-0 silk suture on a small curved needle was passed around the anterolateral branch of the coronary artery, and the ends of the suture were passed through a small vinyl tube to make a snare. Myocardial ischemia was confirmed by ST-segment elevation on the ECG and regional cyanosis of the myocardial surface. Reperfusion was confirmed by a myocardial blush over the risk area after releasing the snare. The surgical wound was closed, and the rabbits were extubated. After 2 days, 2 weeks, or 4 weeks, the rabbits were reanesthetized and intubated, and the incisions were opened. They were then killed with an overdose of pentobarbital sodium. Their hearts were excised and mounted on Langendorff apparatus. The coronary branch was reoccluded, and Monastral Blue dye (4%, Sigma Chemical Co) was injected from the aorta at 80 mm Hg to detect the ischemic risk area.

The ventricular portion of the heart was transversely cut into five slices, each of which was weighed and photographed. In one slice, ischemic and nonischemic areas were isolated using dye perfusion as a guide, and then the slice was frozen in liquid nitrogen and stored at -70°C . The other slices were fixed with 10% buffered formalin after an immediate sampling of small portions of the infarct tissue from the area at risk and noninfarct tissue from the nonischemic area for electron microscopy.

Other main organs such as the lungs, liver, and kidneys were fixed with 10% buffered formalin for the histological examination.

Histology and Immunohistochemistry

The ventricular slices fixed with 10% buffered formalin were embedded in paraffin. After deparaffinization and rehydration, 4- μm -thick sections were stained with hematoxylin-eosin and Masson's trichrome. MI at each phase was histologically confirmed in these sections. In the group with 2-day MI, the MI size was quantified according to a method previously reported.¹⁶ In short, the area at risk (area without blue dye) was identified and traced from an enlarged projection of the photographic slide of each ventricular slice. Next, infarcts were traced on projections of the microscopic slide with Masson's trichrome stain. Since the rabbits were allowed to live for 48 hours after the reperfusion, coagulation necrosis and contraction band necrosis of myocytes and leukocyte infiltration were evident in the infarcted myocardium. This allowed the accurate tracing of infarcted areas even under a relatively low magnification. The area at risk and the infarcted area were quantified by retracing these tracings on a digitizing tablet interfaced to a personal computer. The calculated percentages of the area at risk and the infarcted area of each slice were multiplied by the slice weight and summed to obtain the total tissue weight of area at risk and infarction.

Immunohistochemical reactions were obtained according to an indirect immunoperoxidase method on serial sections from the myocardial slices. After deparaffinization, intrinsic peroxidase activity was inhibited by the addition of 0.3% hydrogen peroxide in methanol, and nonspecific binding was blocked with 5% normal goat serum. The sections were then stained with mouse monoclonal antibodies against rabbit α -sarcomeric actin (α -Sr-1, DAKO Co) at a dilution of 1:50, α -smooth muscle actin (1A4, DAKO) at 1:50, rabbit macrophage (RAM11, DAKO) at 1:50, and human endothelial cell (CD31, DAKO) at 1:100. The slides were incubated overnight at 4°C . For the retrieval of the endothelial cell antigen, treatment with proteinase K (400 $\mu\text{g}/\text{mL}$) for 10 minutes was performed after incubation with hydrogen peroxide. In the second step, the sections were incubated with the peroxidase-conjugated $\text{F}(\text{ab}')_2$ fragment of the secondary antibody [goat anti-mouse IgG(H+L), Jackson ImmunoResearch Laboratories] at a dilution of 1:500 for 30 minutes at room temperature. Immunostains were visualized using diaminobenzidine/hydrogen peroxide. Between all steps, the slides were washed with PBS. Irrelevant mouse IgG was the primary antibody used for the control experiments.

In Situ Detection of Nuclear DNA Fragmentation (TUNEL)

DNA fragments were determined in deparaffinized 4- μm -thick sections from a transverse tissue block by using an ApopTag in situ apoptosis detection kit (Oncor). The DNA nick was labeled according to the supplier's instructions, which are based on the method described by Schmitz et al.¹⁷ After TUNEL, sections were counterstained by being immersed in hematoxylin. Prostate tissue from a rabbit castrated 2 days before study was the positive control for the TUNEL reaction.^{1,18}

Double Immunohistochemistry for TUNEL and Cell-Specific Proteins

For double immunohistochemical analysis, sections were stained first with TUNEL as described above. After incubation with diaminobenzidine substrate, they were washed with PBS. The Vectastain Elite ABC system (Vector Laboratories) was used for the second immunohistochemical analysis. The sections were blocked with 5% horse serum and then incubated with the second primary antibodies (against α -smooth muscle actin [1A4], macrophage [RAM11], or endothelial cell [CD31]; DAKO) that were visualized with VIP substrate (Vector). For the retrieval of the endothelial cell antigen, treatment with proteinase K (100 $\mu\text{g}/\text{mL}$) for 25 minutes was performed before the incubation with the primary antibody.

Morphometrical Analysis of Myocardial Interstitial Cells

Interstitial cells in the infarcted area were counted under a light microscope. In each specimen, the noncardiomyocytes with counterstained nuclei were counted in 20 random HPFs ($\times 400$) in the infarcted area. However, the histological appearance 2 days after MI was quite different between the center of the MI, consisting mainly of dead cardiomyocytes, and the periphery, consisting of infiltrated inflammatory cells in the infarcted area. Therefore, the cells in each area were counted separately in this group. The periphery and center of the infarct 2 days after MI were defined as regions where dead cardiomyocytes were absorbed or not, respectively. Simultaneously, interstitial cell types were identified and classified into leukocytes, macrophages, endothelial cells, vascular smooth muscle cells, myofibroblasts, fibroblasts, and others and/or unclassified cells. The classification was determined basically on the sections stained with hematoxylin-eosin or Masson's trichrome with reference to the immunohistochemical preparations.

Cells in which the nucleus was obviously labeled with diaminobenzidine were defined as TUNEL-positive, and they were also counted. The percentage of the TUNEL-positive to the total cells was then calculated. We then tried to determine the cell types among the TUNEL-positive interstitial cells by the classification system mentioned above. For this, TUNEL and double immunohistochemical preparations were used. The percentages of the interstitial cell types with positive TUNEL occupying the infarcted area were then calculated in each phase of MI. The salvaged myocytes showing a positive TUNEL reaction were also quantified in every group.

DNA Extraction and Electrophoresis

Frozen tissue was minced while being thawed in lysis buffer containing 10% SDS, 10 mmol/L Tris, and 1 mmol/L EDTA (pH 7.8) and digested in lysis buffer with 0.2 mg/mL proteinase K for 17 hours at 37°C. DNA was extracted with phenol/chloroform, and 4 μ g of the DNA was resolved by electrophoresis on a 2.0% agarose gel. The DNA was then visualized with ethidium bromide.

Electron Microscopy

Tissue samples taken from infarcted and noninfarcted areas were cut into 1-mm cubes and fixed for 4 hours at 4°C in 2.5% glutaraldehyde in 0.1 mol/L phosphate buffer. They were postfixed in 1% buffered osmium tetroxide, dehydrated through graded ethanols, and embedded in epoxy resin. Thin sections (80 nm) were cut with a diamond knife, collected on 300-mesh copper or nickel grids, and double-stained with uranyl acetate and lead citrate before examination using an electron microscope (H-700, Hitachi).

Electron Microscopic TUNEL

Electron microscopic TUNEL was performed in accordance with essentially the same principles as reported by Migheli et al.,¹⁹ but with substantial modifications as follows. The fragmented DNA in thin sections on bare 300-mesh nickel grids was labeled using components of the ApopTag kit. After stopping the enzymatic reaction of TdT, the grids were incubated with anti-digoxigenin mouse monoclonal antibody (0.4 μ g/mL IgG, Boehringer Mannheim) for 30 minutes at room temperature. Next, they were incubated with 15 nm gold-labeled goat anti-mouse IgG (Amersham) at a dilution of 1:50 in PBS for 1 hour at room temperature. The grids were then washed with PBS, rinsed in distilled water, counterstained with uranyl acetate and lead citrate, and examined using an electron microscope. The grids were washed with PBS between each step. The validity of this method was checked by omitting TdT during the procedure as the negative control and by using prostate tissue from a rabbit castrated 2 days before as the positive control.^{1,18}

Statistical Analysis

Data are shown as mean \pm SD. The significance of differences in the data was evaluated by one-way ANOVA followed by the Newman-Keuls multiple comparison test. A difference of $P < 0.05$ was considered significant.

Results

Histological and Immunohistochemical Characterization of the Cells Appearing in Postinfarct Tissues

A number of acute inflammatory cells infiltrated the infarcted tissue, and red blood cells were frequently seen, especially in the peripheral zone at 2 days after MI. Inflammatory cells included both polymorphonuclear and mononuclear leukocytes. Cells positive for α -smooth muscle-specific actin were restricted to the vasculature (Figure 1). Dead cardiomyocytes were visible in the central zone of the infarcted area. All of the infarcted cardiomyocytes were severely degenerated and had lost the antigenicity of α -sarcomeric actin. The nuclei had already disappeared in most of the infarcted cardiomyocytes. The infarct size as a percentage of the area at risk was $40.2 \pm 6.7\%$, and infarct size as a percentage of the left ventricle was $9.5 \pm 4.5\%$ (ranging from 4.6% to 17.4%) in the rabbits at 2 days after MI. These values were in accordance with the previous report.¹⁶

At 2 weeks after MI, the leukocytes and dead cardiomyocytes had subsided, and the key histological features in the infarcted area were granulation consisting of fibroblasts, macrophages positive for RAM11, neovascularization positive for CD31, and collagen fibers surrounding the necrotic and partially calcified tissue. There were abundant myofibroblasts that were positive for α -smooth muscle-specific actin (Figure 1). The area positive for α -smooth muscle-specific actin occupied 11.8% to 63.4% (mean \pm SD, $40.6 \pm 16.3\%$) of the 2-week-old infarcted area, as measured by a digitizer connected to a personal computer. Myofibroblasts were oriented in parallel to the salvaged cardiomyocytes at the edges of the infarct. Macrophages were distributed mainly on the edges of necrotic tissue, and some of them formed multinucleate giant cells.

At 4 weeks after MI, the cellularity was markedly decreased in the infarcted area, and a few cells, mainly fibroblasts, were identified as the cellular elements around the center of the infarct, which was replaced by fat or collagen (Figure 1).

No rabbit at any infarct age showed congestion of the lungs, liver, or kidneys.

TUNEL at Light Microscopic Level and Morphometrical Analysis

In the infarcted areas of all 8 of the rabbits at 2 days after MI, a positive TUNEL reaction was constantly and easily noted in acute inflammatory cells under the light microscope (Figure 2). Granulation tissue in the infarcted areas of all 8 of the rabbits at 2 weeks after MI contained TUNEL-positive cells (Figure 2). In all 8 of the rabbits at 4 weeks after MI, when the key feature of the infarcted area was scar formation, TUNEL-positive interstitial cells were also observed, but to a lesser extent than in the rabbits at 2 days and 2 weeks after MI.

The total number of interstitial cells in the infarcted area of the 2-day MI group was 139 ± 35 cells/HPF in the central portion of the MI and 586 ± 34 cells/HPF in the periphery. It was 292 ± 69 cells/HPF in the 2-week MI group and 152 ± 26 cells/HPF in the 4-week MI group. Thus, the cell population

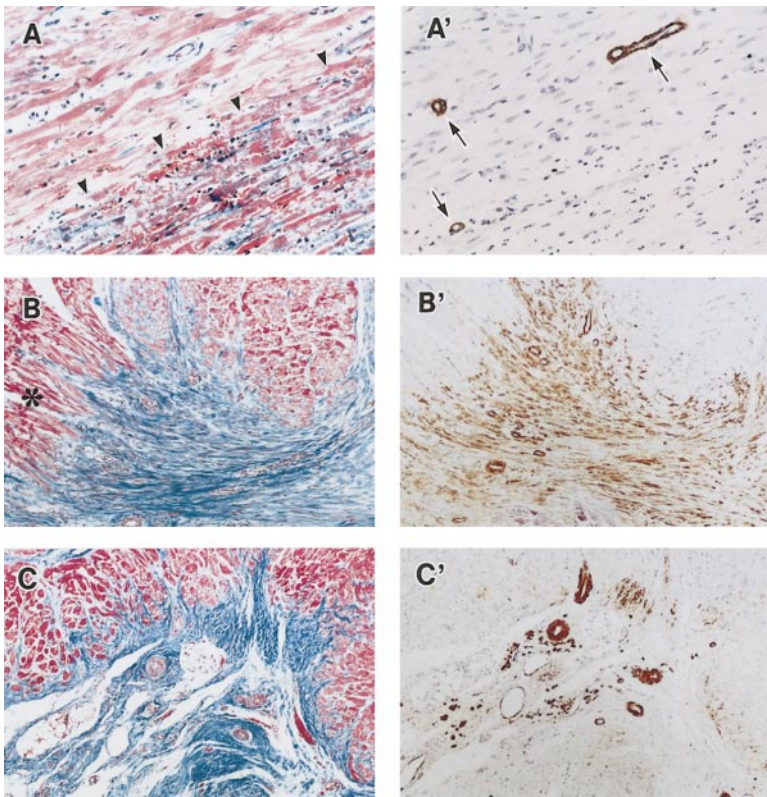


Figure 1. Photomicrographs showing the time course of rabbit MI revealed by Masson's trichrome stain (left panels) and immunohistochemical reactions against α -smooth muscle-specific actin on the serial sections (right panels). A and A', 2-day MI. B and B', 2-week MI. C and C', 4-week MI. Panel A shows histological findings of acute 2-day MI. The upper half shows salvaged tissues, and the lower half shows infarcted tissues. The arrowheads mark the border of MI. Panels B and C represent the granulation tissue of 2-week MI and scar tissue of 4-week MI, respectively, stained blue. In panel A', brown α -smooth muscle actin was restricted to the vasculature (arrows) in 2-day MI. However, there were abundant myofibroblasts that were positive for α -smooth muscle-specific actin in granulation tissue (panel B'). Myofibroblasts in panel (B') are oriented in parallel to the salvaged cardiomyocytes indicated by asterisks in panel B. The myofibroblasts had become rare but were still noted in scar tissue (panel C'). Original magnifications, $\times 100$ (panels A and A') and $\times 40$ (panels B, B', C, and C').

significantly decreased as the healing of the MI progressed (Figure 3A, upper panel). The main constituents of the interstitial cells were leukocytes ($61.3 \pm 12.5\%$ [85.1 ± 17.4 cells/HPF] in the center and $75.0 \pm 4.6\%$ [439.4 ± 26.9 cells/HPF] in the periphery of the infarcted area) at 2 days after MI, myofibroblasts ($32.5 \pm 13.4\%$ [94.9 ± 39.1 cells/HPF]), macrophages ($29.4 \pm 11.8\%$ [85.8 ± 34.5 cells/HPF]), and endothelial cells ($17.5 \pm 4.6\%$ [51.1 ± 13.4 cells/HPF]) at 2 weeks after MI, and fibroblasts ($49.1 \pm 15.9\%$ [74.5 ± 24.1 cells/HPF]) at 4 weeks after MI (Figure 3A, lower panel).

The mean incidence of TUNEL-positive interstitial cells was significantly higher in the center ($5.3 \pm 3.6\%$) and the periphery ($6.9 \pm 3.3\%$) of the 2-day MI group compared with the 2-week ($2.5 \pm 1.0\%$) and 4-week ($0.5 \pm 0.5\%$) MI groups (Figure 3B, upper panel). The proportion of each cell type with positive TUNEL was in accordance with that of the whole count of each cell type (Figure 3B, lower panel): the main constituents of the TUNEL-positive interstitial cells were leukocytes ($61.3 \pm 12.5\%$ [2.8 ± 0.7 cells/HPF] in the center and $75.0 \pm 4.6\%$ [21.8 ± 3.6 cells/HPF] in the periphery

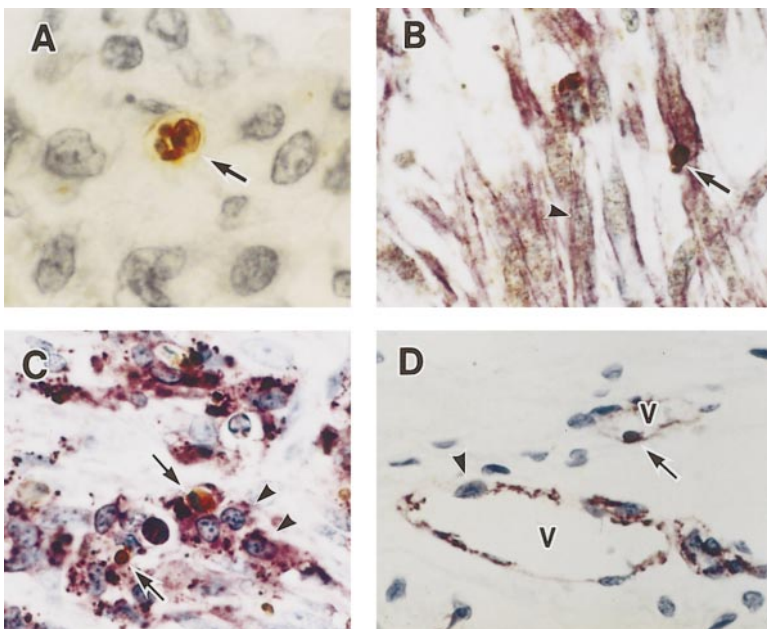


Figure 2. Positive TUNEL reactions observed in various types of cells after MI. A, A polymorphonuclear leukocyte with positive TUNEL reaction (indicated by an arrow; ie, stained brown) in infarcted area 2 days after MI. B, Double immunohistochemical preparation (α -smooth muscle-specific actin and TUNEL) of the infarct tissue 2 weeks after MI. The myofibroblasts were positive for α -smooth muscle-specific actin (purple cytoplasm). A myofibroblast double-positive for TUNEL (brown nucleus indicated by an arrow) and α -smooth muscle-specific actin is seen. A myofibroblast negative for TUNEL is indicated by an arrowhead. C, Macrophages double-positive for TUNEL (brown nucleus) and RAM11 (purple cytoplasm) 2 weeks after MI (indicated by arrows). Macrophages (arrowheads, positive for RAM11) are negative for TUNEL. D, A capillary endothelial cell double-positive for TUNEL and CD31 2 weeks after MI (arrow). Endothelial cells (arrowhead) are negative for TUNEL. V indicates vessel lumen. Original magnifications, $\times 750$ (A) and $\times 400$ (B through D).

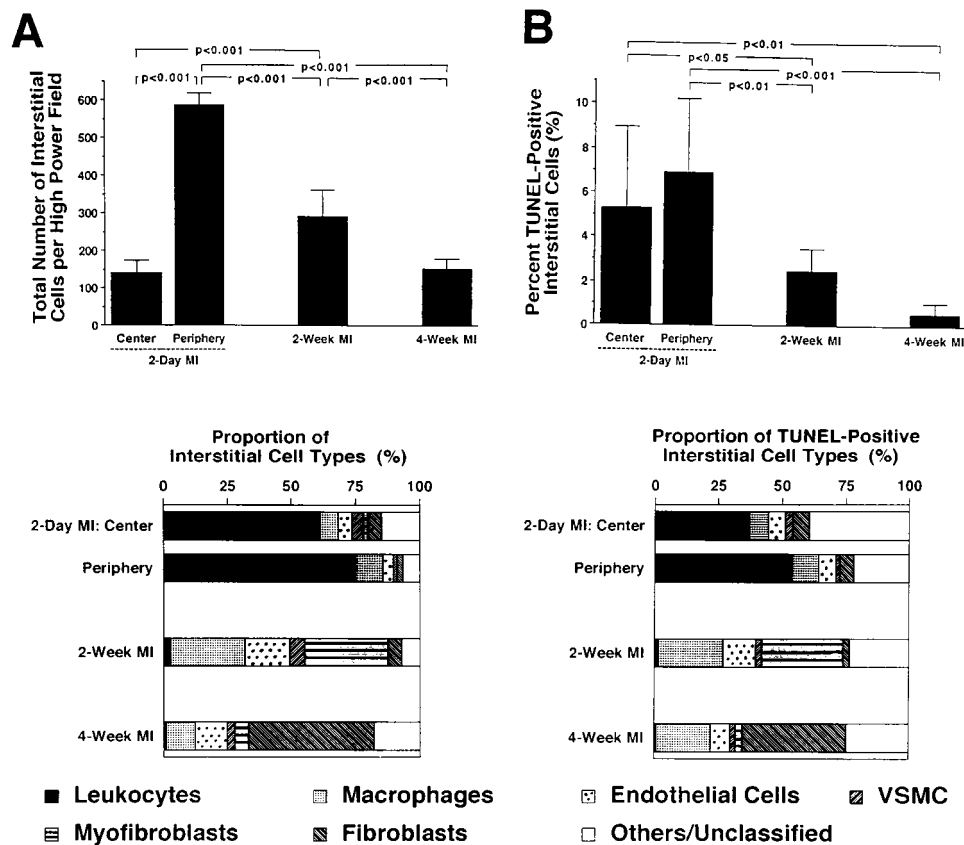


Figure 3. A, Total number of interstitial cells (noncardiomyocytes) per HPF ($\times 400$) in the infarcted area 2 days, 2 weeks, and 4 weeks after MI (top) and proportion of interstitial cell types occupying the infarcted area expressed as a percentage (bottom). B, Mean incidence of TUNEL-positive interstitial cells in the infarcted area 2 days, 2 weeks, and 4 weeks after MI (top) and proportion of TUNEL-positive interstitial cell types in the infarcted area expressed as a percentage (bottom). VSMC indicates vascular smooth muscle cells.

of the infarcted area) at 2 days after MI, myofibroblasts ($32.5 \pm 13.4\%$ [2.3 ± 0.2 cells/HPF]) and macrophages ($29.4 \pm 11.8\%$ [2.1 ± 0.8 cells/HPF]) at 2 weeks after MI, and fibroblasts ($49.1 \pm 15.9\%$ [0.4 ± 0.1 cells/HPF]) at 4 weeks after MI. However, for many of the cells with positive TUNEL, it was difficult to identify their cell types because of the shriveled cytoplasm or cellular fragmentation. Thus, the proportion of others/unclassified cells was substantial in all groups.

The salvaged cardiomyocytes with a positive TUNEL reaction were extremely rare ($<0.01\%$) at each stage after MI, and their incidence in the infarct border was similar to that seen in the nonischemic areas.

DNA Agarose Gel Electrophoresis

Tissues of infarcted areas obtained from all 8 of the rabbits at 2 days after MI contained fragmented DNA that produced a ladder of DNA bands representing integer multiples of internucleosomal DNA length (≈ 180 bp) (Figure 4). The ladder was never seen in tissues from the nonischemic areas of any of the rabbits or in tissues of the infarcted areas from any of the rabbits at 2 and 4 weeks after MI (Figure 4).

Electron Microscopy

At 2 days after MI, many apoptotic leukocytes were scattered among the nonapoptotic leukocytes (Figure 5). They showed distinct morphological features of apoptosis, such as the

eccentric margination of nuclear chromatin, the extreme condensation of chromatin, and densely compacted cytoplasm. Their plasma membranes were not disrupted. However, leukocytes with necrotic findings such as cytoplasmic swelling and a disrupted plasma membrane were rare. At the

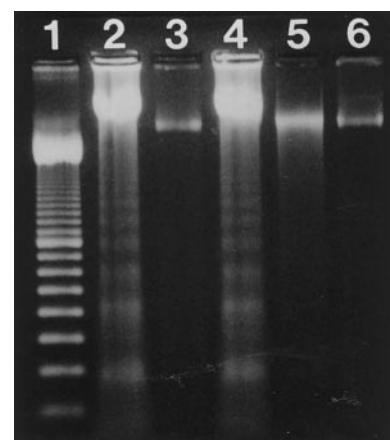


Figure 4. Agarose gel electrophoresis of DNA. Lane 1 is a 100-bp ladder marker. Lane 2 is from the prostate of a rabbit castrated 2 days before study and used as a positive control. Lanes 3 and 4 are from a rabbit heart 2 days after MI (lane 3, nonischemic area; lane 4, ischemic area). Lane 5 is from the ischemic area of a heart 2 weeks after MI. Lane 6 is from the ischemic area of a heart 4 weeks after MI. Note that the ischemic area of the 2-day MI (lane 4) shows a clear ladder.

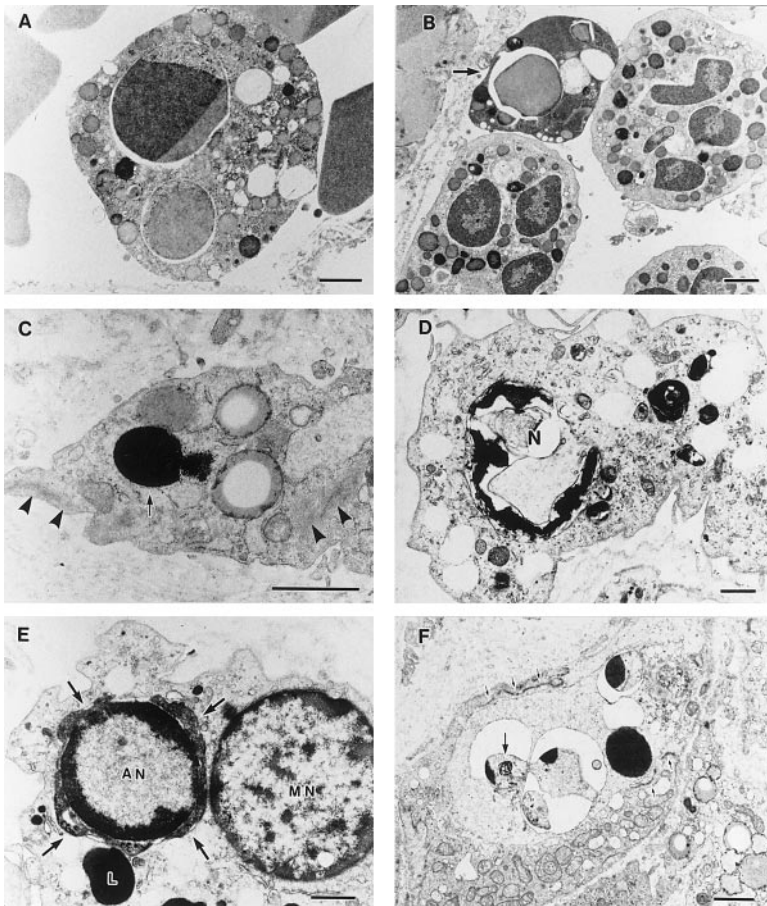


Figure 5. Electron micrographs showing myocardial interstitial cell apoptosis in infarcted areas: inflammatory cells in 2-day MI (A and B) and granulation tissue in 2-week MI (C through F). A and B, Nuclear chromatin is eccentric in the leukocyte shown in panel A and markedly condensed in panel B. An apoptotic leukocyte is indicated by the arrow in panel B, in which not only nuclei but also the cytoplasm are markedly shrunken. The plasma membrane in each apoptotic cell is not ruptured. C, A typically apoptotic myofibroblast. The homogeneously condensed nucleus with a glossy appearance is indicated by an arrow, and the intracytoplasmic microfilaments are indicated by arrowheads. D, An apoptotic macrophage. The nucleus with peripherally condensed chromatin is seen in the center (N), and many phagolysosomes are noted in the cytoplasm. E, An apoptotic cell (surrounded by arrows) engulfed by a macrophage, in which severely shrunken cytoplasm surrounds the nucleus with marginally condensed chromatin. AN indicates nucleus of apoptotic cell; MN, nucleus of the macrophage; and L, lipid droplet in the macrophage. F, An apoptotic cell of unknown origin with figures of apoptotic bodies surrounded by endothelial cells. Small arrows indicate cellular junctions of the endothelial cells. The remains of the nucleolus (larger arrow) are evident in one of the apoptotic bodies. Bars=1 μ m.

same time, all of the dead cardiomyocytes (detached from the basal lamina) in the infarcted areas had ragged myofibrils, swollen mitochondria with amorphous dense bodies, and a definitely ruptured plasma membrane. Most of the nuclei were cleared in the center, in which clumped chromatin with various sizes was margined and scattered. These were electron microscopic findings of the necrotic death of cardiomyocytes.

In granulation tissue at 2 weeks after MI, typical apoptosis was evident in many myofibroblasts containing microfilament bundles with dense bodies. The margination of chromatin and the dilatation of endoplasmic reticulum, sometimes accompanied by a marked condensation of chromatin and the formation of nuclear fragments surrounded or not by a membrane, were observed; no disruption of plasma membranes was seen. In addition, many macrophages contained phagolysosomes. The contents of the phagolysosomes were apparently apoptotic bodies in some macrophages. Macrophages undergoing apoptosis were also observed. Apoptosis was seen in capillary endothelial cells. In addition to the cells with typical apoptotic figures, we identified other myofibroblasts, macrophages, and capillary endothelial cells that contained nuclei with homogeneous density but without marked condensation. These cells had a slightly enlarged endoplasmic reticulum and intact plasma membranes, appearing neither normal nor necrotic. On the other hand, myofibroblasts and macrophages with typical necrotic findings were rare. In scar tissue at 4 weeks after MI, the apoptotic

figures in myofibroblasts and macrophages were similar, but the incidence was extremely rare. There was no evidence of an apoptotic ultrastructure in the salvaged cardiomyocytes at each stage after MI.

Electron Microscopic TUNEL

The methodological validity of the TUNEL staining at the electron microscopic level was first evaluated on the sections of castrated rabbit prostate. Fragmented DNA labeled with gold tended to accumulate slightly on nuclear chromatin even in the apparently normal cells, but the accumulation was so marked on the margined or condensed chromatin of apoptotic cells that we easily identified the nuclei of apoptotic cells (Figure 6A and 6B). When TdT was omitted during the staining procedure, gold particles did not accumulate in any cells.

Immunogold particles labeled the nuclei of typically apoptotic leukocytes, myofibroblasts, endothelial cells, and apoptotic bodies engulfed by macrophages. They were also accumulated on other interstitial cells with the nuclei showing homogeneous density but not such severe condensation as that of typical apoptotic nuclei. The nuclei of apparently normal cells were only slightly accumulated by gold particles, and other subcellular organelles of both apoptotic and non-apoptotic cells were never labeled.

Discussion

The present study revealed the apoptosis of many interstitial cells during the healing process of MI in rabbits.

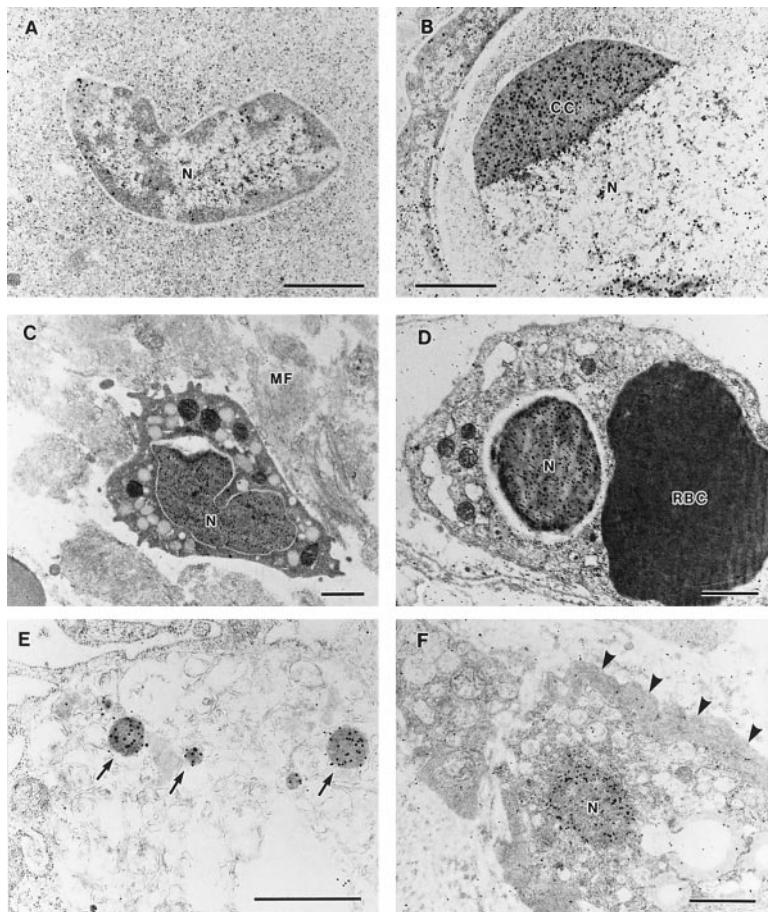


Figure 6. Electron micrographs of preparations labeled with immunogold for electron microscopic TUNEL. A and B, Normal (panel A) and apoptotic (panel B) cells of the prostate are shown from a rabbit castrated 2 days before study. Gold particles are accumulated slightly on the nucleus (N, panel A) of a normal cell but much more on the condensed chromatin (CC) of the nucleus (N, panel B) of an apoptotic cell. Gold particles are rare on other subcellular structures. C, An apoptotic leukocyte. Numerous gold particles label the condensed nucleus (N). MF indicates myofibrils of the infarcted cardiomyocyte. D, Condensed nucleus (N) of a capillary endothelial cell is definitely labeled by gold particles. RBC indicates red blood cell in the capillary lumen. E, Engulfed electron-dense materials (indicated by arrows) are labeled by gold particles and are therefore TUNEL-positive. They are thus thought to be apoptotic bodies. F, The nucleus (N) of a myofibroblast is markedly labeled by gold particles. This cell is not typical of an apoptotic cell, but its nucleus shows homogeneous density. Arrows indicate microfilaments in the myofibroblast. Bars = 1 μ m.

Apoptosis in Interstitial Cells After MI

In the present study, DNA ladders were detected in 2-day MI but not in 2- and 4-week MI. TUNEL-positive interstitial cells at the light microscopic level were lesser in number in the 2-week and 4-week MI than in the 2-day MI. The electron microscopic analysis confirmed this finding. DNA ladders are generally reliable as a marker of apoptosis^{14,15}; however, this method has the disadvantage of low sensitivity. DNA degradation is detectable by this method only when a high proportion of apoptotic cells is present.^{20,21} The lack of DNA ladders in the present 2- and 4-week MI could be explained by the low sensitivity of the method.

In the present study, the percentage of TUNEL-positive cells at the light microscopic level was 5% to 7% during the acute stage and 2.5% at the granulation stage, which appeared relatively low. However, the morphological changes of apoptosis occur within minutes, as shown by videomicroscopy.²² Therefore, the incidence of TUNEL-positive cells in the present study might be sufficient for a decrease in cellularity. Interstitial cells showing the ultrastructure of necrosis were few in the present study. Thus, apoptosis appears to have mediated the decrease in cellularity during the transition both between acute inflammatory cell infiltration and granulation tissue and between granulation tissue and scar deposition after MI.

Apoptotic cell death could be classified into two phases in the present study: (1) leukocytes at the acute inflammatory phase and (2) myofibroblasts, endothelial cells, and macro-

phages at the granulation tissue phase. It has been reported that leukocytes undergo apoptosis in culture and in organs such as the lungs.^{23–25} Cheng et al¹³ reported TUNEL-positive interstitial cells and capillary endothelial cells in infarcted myocardium in rats. Desmoulière et al²¹ found evidence of apoptosis in granulation tissue in an experimental traumatic injury of rat skin. We recently reported that Bcl-2 and Bax, apoptosis-related factors, are expressed in the inflammatory cells after MI in humans.¹¹ These findings suggest that apoptosis is a general removal mechanism of acute and chronic inflammatory cells.

Pathophysiological Role of Apoptosis in Infiltrated Leukocytes and Proliferated Interstitial Cells After MI

Generally, the accumulation of leukocytes and the subsequent proliferation of granulation tissue cells are inflammatory responses against the necrosis of cardiomyocytes. The fate of leukocytes infiltrated into the infarcted myocardial tissue is not yet known. The results of the present study showed their elimination via apoptosis. This observation seems to reflect well one of the representative roles of apoptosis: purposeful suicide by cells. Leukocytes and macrophages have various cytokines, proteases, and other factors that are cytotoxic; thus, when these cells die in situ, they should be expected to be removed by apoptosis, not by necrosis (during which the cellular contents are released and may induce excessive or prolonged inflammation).

Myofibroblasts are characteristic interstitial spindle-shaped cells appearing in granulation tissue; they share characteristics of both fibroblasts and smooth muscle cells.²⁶ Characteristic ultrastructural features of myofibroblasts are the presence of stress fibers with subplasmalemmal attachment plaques and abundant rough endoplasmic reticulum with an adjacent discontinuous deposition of basal lamina-like material and intracytoplasmic filaments.^{27,28} Myofibroblasts show an immunohistochemical expression of α -smooth muscle-specific actin.²⁹ Myofibroblasts have been identified in rat³⁰ and human³¹ MI. In the present study, we found numerous myofibroblasts in granulation tissue after MI in rabbits. The pathophysiological significance of such a massive appearance (up to 40% of the infarcted area) and a subsequent decrease of myofibroblasts during the healing of MI remains unknown. Collagen synthesis may be one of the important roles of myofibroblasts, supplementing the damaged area where parenchymal tissue is defective (scar formation).^{26,32} Moreover, since cardiac ventricles are exposed to hemodynamic stress, high numbers of myofibroblasts may be needed as transient tissue reinforcement until a hard scar is established. Thus, the appearance of so many myofibroblasts seems to be an adaptive response specific to myocardial tissue.

The massive proliferation of myofibroblasts and their disappearance via apoptosis imply the significant participation of myofibroblasts in ventricular remodeling after MI. In this regard, modulation of the myofibroblast population would make room for therapeutic interventions during the healing stages of MI, since abnormal remodeling is one of the important problems for the postinfarct heart, perhaps causing heart failure. However, we do not yet know whether the blockade or acceleration of myofibroblast apoptosis would be beneficial or harmful. That is, making scar tissues collagen-rich and thus stronger by blocking apoptosis in myofibroblasts, which synthesize collagen,^{26,32} may prevent excessive ventricular dilatation or may cause prolongation of fragile granulation tissues. Conversely, decreasing myocardial fibrosis by accelerating apoptosis may prevent abnormal remodeling by suppressing excessive fibrosis or may cause aneurysmal expansion due to a lack of sturdy connective tissues. Further investigations are warranted.

Simultaneous Observation of Ultrastructure of Apoptotic Cells and DNA Fragmentation by Electron Microscopic TUNEL Method

Migheli et al¹⁹ recently applied the TUNEL method at the electron microscopic level in neural cells and reported that the characteristic ultrastructural features of apoptosis were directly associated with DNA fragmentation. In our present study, each nucleus of the myocardial interstitial cells with typical apoptotic ultrastructures had a marked accumulation of immunogold particles, indicating DNA fragmentation. Conversely, immunogold particles were markedly accumulated even in the nuclei of cells that showed neither typically apoptotic nor normal ultrastructures. The atypical ultrastructures with DNA fragmentation may indicate an early stage of apoptosis. In addition, the nuclear chromatin of the cells with a normal ultrastructure was slightly labeled with immunogold. Possible explanations for this are a small amount of

cleaved DNA even in the apparently normal cells or little cleavage of DNA as an artificial product during tissue processing.

Apoptosis in Infarcted and Salvaged Cardiomyocytes

Apoptosis has been reported in the infarcted myocytes after acute MI.⁴⁻¹⁰ Especially, TUNEL-positive myocytes were frequently seen in rabbit hearts that underwent a 30-minute occlusion of the coronary artery and then a 4-hour reperfusion.⁷ In the present study, in hearts of rabbits subjected to the 2-day reperfusion after 30 minutes of occlusion (the earliest time point examined), the infarcted myocytes showed severe degeneration, and the nuclei had already disappeared in most of the infarcted myocytes at the light and electron microscopic levels. This indicates that 2-day reperfusion after 30-minute occlusion is too late to define the relation between infarcted myocytes and apoptosis. Therefore, we did not evaluate apoptosis in the infarcted myocytes in the present study.

In the salvaged myocytes surrounding the old MI, TUNEL-positive myocytes were light- and electron-microscopically rare in the rabbit hearts with 2-week and 4-week reperfusion after 30-minute occlusion in the present study. These data differed from those of previous studies indicating the presence of apoptotic myocytes.^{12,13} The animal species were dogs in the study by Sharov et al¹² and rats in the study by Cheng et al.¹³ Sharov et al studied multiple infarctions due to embolism of small coronary arteries induced by the injection of numerous microspheres; Cheng et al studied very large infarctions due to a permanent coronary arterial occlusion (the infarct size of which was reported to be $\approx 63\%$ of the left ventricular free wall in an earlier study using the same experimental rat model³³). Both studies showed definite congestive heart failure. Recently, the presence of apoptotic myocytes was reported in congestive heart failure with dilated cardiomyopathy.^{34,35} In the present study using rabbits reperused after 30 minutes of coronary occlusion, the infarct size was not extensive ($9.5 \pm 4.5\%$, ranging from 4.6% to 17.4% of the left ventricle). It is well known that chronic congestive heart failure is generally seen in large myocardial infarctions (measuring $>20\%$ to 25% of the left ventricle).³⁶ In addition, there was no pathological evidence in the present model of congestion in the lungs or liver, indicating the absence of congestive heart failure. Therefore, the discrepancy between the previous and present studies regarding apoptotic myocytes in hearts with an old MI would be explained by the differences in models with and without congestive heart failure.

Conclusions

Many apoptotic cells were found in acute inflammatory and granulation tissues after MI in rabbits. Thus, apoptosis played an important role in the disappearance of the infiltrated and proliferated myocardial interstitial cells after MI. Because apoptosis represents a potentially inducible or preventable form of cell death, this finding may imply therapeutic applications of apoptosis management (its acceleration or blockade) to postinfarct ventricular remodeling. Electron

microscopy combined with TUNEL showed that the characteristic ultrastructure of apoptotic nuclei reflects DNA fragmentation but that not all of the cells with DNA fragmentation are typically apoptotic in ultrastructure.

Acknowledgments

This study was supported in part by research grants 017457598, 1995; 08457204, 1996; 08670831, 1996; and 09470165, 1997, from the Ministry of Education, Science, and Culture of Japan. Thanks are due to Toshie Ohtsubo, Akiko Hara, Rumi Maruyama, Kaoru Kuroiwa, Noriko Ishida, Tomoko Sugita, Yuki Shimomura, Reiko Nitta, Yasuko Saika, Yuka Kitagawa, and Kanako Nakajima for their technical assistance with the histochemistry and to Mika Itoh for her secretarial assistance. We are indebted to Toshihiko Okumura for his advice regarding electron microscopy and Daniel Mrozek for reading the manuscript.

References

- Kerr JFR, Wyllie AH, Currie AR. Apoptosis: a basic biological phenomenon with wide-ranging implications in tissue kinetics. *Br J Cancer*. 1972;26:239–257.
- Wyllie AH, Kerr JFR, Currie AR. Cell death: the significance of apoptosis. *Int Rev Cytol*. 1980;68:251–306.
- Searle J, Kerr JF, Bishop CJ. Necrosis and apoptosis: distinct modes of cell death with fundamentally different significance. *Pathol Annu*. 1982;17(pt 2):229–259.
- Itoh G, Tamura J, Suzuki M, Suzuki Y, Ikeda H, Koike M, Nomura M, Jie T, Ito K. DNA fragmentation of human infarcted myocardial cells demonstrated by the nick end labeling method and DNA agarose gel electrophoresis. *Am J Pathol*. 1995;146:1325–1331.
- Bardales RH, Hailey LS, Xie SS, Schaefer RF, Hsu SM. In situ apoptosis assay for the detection of early acute myocardial infarction. *Am J Pathol*. 1996;149:821–829.
- Saraste A, Pulkki K, Kallajoki M, Henricksen K, Parvinen M, Voipio-Pulkki L-M. Apoptosis in human acute myocardial infarction. *Circulation*. 1997;95:320–323.
- Gottlieb RA, Bursleson KO, Kloner RA, Babior BM, Engler RL. Reperfusion injury induced apoptosis in rabbit cardiomyocytes. *J Clin Invest*. 1994;94:1621–1628.
- Buerke M, Murohara T, Skurk C, Nuss C, Tomaselli K, Lefer AM. Cardioprotective effect of insulin-like growth factor I in myocardial ischemia followed by reperfusion. *Proc Natl Acad Sci USA*. 1995;92:8031–8035.
- Kajstura J, Cheng W, Reiss K, Clark WA, Sonnenblick EH, Krajewski S, Reed JC, Olivetti G, Anversa P. Apoptotic and necrotic myocyte cell deaths are independent contributing variables of infarct size in rats. *Lab Invest*. 1996;74:86–107.
- Fliss H, Gattlinger D. Apoptosis in ischemic and reperfused rat myocardium. *Circ Res*. 1996;79:949–956.
- Misao J, Hayakawa Y, Ohno M, Kato S, Fujiwara T, Fujiwara H. Expression of bcl-2 protein, an inhibitor of apoptosis, and Bax, an accelerator of apoptosis, in ventricular myocytes of humans with myocardial infarction. *Circulation*. 1996;94:1506–1512.
- Sharov VG, Sabbah HN, Shimoyama H, Goussev AV, Lesch M, Goldstein S. Evidence of cardiocyte apoptosis in myocardium of dogs with chronic heart failure. *Am J Pathol*. 1996;148:141–149.
- Cheng W, Kajstura J, Nitahara JA, Li B, Reiss K, Liu Y, Clark WA, Krajewski S, Reed JC, Olivetti G, Anversa P. Programmed myocyte cell death affects the viable myocardium after infarction in rats. *Exp Cell Res*. 1996;226:316–327.
- Wyllie AH. Glucocorticoid-induced thymocyte apoptosis is associated with endogenous endonuclease activation. *Nature*. 1980;284:555–556.
- Arends MJ, Morris RG, Wyllie AH. Apoptosis: the role of the endonuclease. *Am J Pathol*. 1990;136:593–608.
- Tanaka M, Fujiwara H, Yamazaki K, Sasayama S. Superoxide dismutase and N-2-mercaptopyrionyl glycine attenuate infarct size limitation effect of ischaemic preconditioning in the rabbit. *Cardiovasc Res*. 1994;28:980–986.
- Schmitz GG, Walter T, Seibl R, Kessler C. Nonradioactive labeling of oligonucleotides in vitro with the hapten digoxigenin by tailing with terminal transferase. *Anal Biochem*. 1991;192:222–231.
- Wijmsman JH, Jonker RR, Keijzer R, Van de Velde CJH, Cornelisse CJ, Van Dierendonck JH. A new method to detect apoptosis in paraffin sections: in situ end-labeling of fragmented DNA. *J Histochem Cytochem*. 1993;41:7–12.
- Migheli A, Attanasio A, Schiffer D. Ultrastructural detection of DNA strand breaks in apoptotic neural cells by in situ end-labeling techniques. *J Pathol*. 1995;176:27–35.
- Rotello RJ, Hocker MB, Gerschenson LE. Biochemical evidence for programmed cell death in rabbit uterine epithelium. *Am J Pathol*. 1989;134:491–495.
- Desmoulière A, Redard M, Darby I, Gabbiani G. Apoptosis mediates the decrease in cellularity during the transition between granulation tissue and scar. *Am J Pathol*. 1995;146:56–66.
- Evan GI, Wyllie AH, Gilbert CS, Littlewood TD, Land H, Brooks M, Waters CM, Penn LZ, Hancock DC. Induction of apoptosis in fibroblasts by c-myc protein. *Cell*. 1992;69:119–128.
- Savill JS, Wyllie AH, Henson JE, Walport MJ, Henson PM, Haslett C. Macrophage phagocytosis of aging neutrophils in inflammation: programmed cell death in the neutrophil leads to its recognition by macrophages. *J Clin Invest*. 1989;83:865–875.
- Grigg JM, Savill JS, Sarraf C, Haslett C, Silverman M. Neutrophil apoptosis and clearance from neonatal lungs. *Lancet*. 1991;338:720–722.
- Savill J, Haslett C. Granulocyte clearance by apoptosis in the resolution of inflammation. *Semin Cell Biol*. 1995;6:385–393.
- Gabbiani G, Ryan GB, Majno G. Presence of modified fibroblasts in granulation tissue and their possible role in wound contraction. *Experientia*. 1971;27:549–550.
- Ghadially FN. Myofibroblasts and myofibroblastoma. In: Ghadially FN, ed. *Ultrastructural Pathology of the Cell and Matrix*. 3rd ed. London, UK: Butterworths; 1988;2:872–877.
- Lipper S, Kahn LB, Reddick RL. The myofibroblast. *Pathol Ann*. 1980;15(pt 1):409–411.
- Skalli O, Schürch W, Seemayer T, Lagace R, Montandon D, Pittet B, Gabbiani G. Myofibroblasts from diverse pathologic settings in their content of actin isoforms and intermediate filament proteins. *Lab Invest*. 1989;60:275–285.
- Vracco R, Thoring D. Contractile cells in rat myocardial scar tissue. *Lab Invest*. 1990;63:21–29.
- Willems IEG, Havenith MG, De Mey JGR, Daemen MJAP. The α -smooth muscle actin-positive cells in healing human myocardial scars. *Am J Pathol*. 1994;145:868–875.
- Schürch W, Seemayer TA, Gabbiani G. Myofibroblast. In: Sternberg SS, ed. *Histology for Pathologists*. New York, NY: Raven Press Publishers; 1992:109–144.
- Olivetti G, Capasso JM, Sonnenblick EH, Anversa P. Side-to-side slippage of myocytes participates in ventricular wall remodeling acutely after myocardial infarction in rats. *Circ Res*. 1990;67:23–34.
- Narula J, Haider N, Virmani R, DiSalvo TG, Kolodige FD, Hajjar RJ, Schmidt U, Semigran MJ, Dec GW, Khaw BA. Apoptosis in myocytes in end-stage heart failure. *N Engl J Med*. 1996;335:1182–1189.
- Olivetti G, Abbi R, Quaini F, Kajstura J, Cheng W, Nitahara JA, Quaini E, Loreto CD, Beltrami CA, Krajewski S, Reed JC, Anversa P. Apoptosis in the failing human heart. *N Engl J Med*. 1997;336:1131–1141.
- Antman EM, Braunwald E. Acute myocardial infarction. In: Braunwald E, ed. *Heart Disease: A Textbook of Cardiovascular Medicine*. Philadelphia, Pa: WB Saunders Co; 1997:1184–1288.

Circulation Research

JOURNAL OF THE AMERICAN HEART ASSOCIATION



Role of Apoptosis in the Disappearance of Infiltrated and Proliferated Interstitial Cells After Myocardial Infarction

Genzou Takemura, Michiya Ohno, Yukihiro Hayakawa, Jun Misao, Motoo Kanoh, Atsuko Ohno, Yoshihiro Uno, Shinya Minatoguchi, Takako Fujiwara and Hisayoshi Fujiwara

Circ Res. 1998;82:1130-1138

doi: 10.1161/01.RES.82.11.1130

Circulation Research is published by the American Heart Association, 7272 Greenville Avenue, Dallas, TX 75231

Copyright © 1998 American Heart Association, Inc. All rights reserved.

Print ISSN: 0009-7330. Online ISSN: 1524-4571

The online version of this article, along with updated information and services, is located on the World Wide Web at:

<http://circres.ahajournals.org/content/82/11/1130>

Permissions: Requests for permissions to reproduce figures, tables, or portions of articles originally published in *Circulation Research* can be obtained via RightsLink, a service of the Copyright Clearance Center, not the Editorial Office. Once the online version of the published article for which permission is being requested is located, click Request Permissions in the middle column of the Web page under Services. Further information about this process is available in the [Permissions and Rights Question and Answer](#) document.

Reprints: Information about reprints can be found online at:
<http://www.lww.com/reprints>

Subscriptions: Information about subscribing to *Circulation Research* is online at:
<http://circres.ahajournals.org/subscriptions/>